

# *In situ* Polarization of Polymer Films in Microsensors

M. Kranz<sup>1</sup>, M.G. Allen<sup>2</sup>, and T. Hudson<sup>3</sup>

<sup>1</sup>EngeniusMicro, LLC., Huntsville, AL, USA

<sup>2</sup>Georgia Institute of Technology, Atlanta, GA, USA

<sup>3</sup>U.S. Army AMRDEC, Huntsville, AL, USA

## ABSTRACT

Electret and polymer piezoelectric films have been previously integrated into Micro Electro Mechanical System (MEMS) acoustic sensors and energy harvesters. Common techniques employed in MEMS polymer integration include corona discharge [1] and backlighted thyatron [2], followed by macro-scale assembly of the polymer into the micro device. In contrast, this paper reports a method for post-fabrication *in-situ* polarization of polymer films embedded within the MEMS device itself. The method utilizes microplasma discharges with self-aligned charging grids integrated within the device to charge fluoropolymer films in a fashion similar to the common corona discharge technique. This *in-situ* approach enables the integration of uncharged polymer films into MEMS and subsequent post-fabrication and post-packaging polarization, simultaneously enabling the formation of buried or encapsulated electrets as well as eliminating the need to restrict fabrication and packaging processes that might otherwise discharge pre-charged materials. Using the *in situ* approach, a microscale charging grid structure is fabricated and suspended a short distance above the polymer film. After fabrication of the charging grid, standard microfabrication steps are performed to build MEMS sensors. After completing the entire fabrication and packaging flow, the polarization process is performed. When energized by a high voltage, the sharp metal edges of the charging grid lead to high dielectric fields that ionize the air in the gap and force electric charge onto the polymer surface. This paper presents modeling and results for this *in situ* polarization process.

**Keywords:** Microplasma, Microcorona, Electret, Ultrasonic

## 1. INTRODUCTION

An electret, the electrostatic analog of a magnet, is a material with a quasi-permanent electrostatic polarization. Electrets can be fabricated from organic or inorganic materials, with polymers including Mylar and Teflon being commonly employed. Films can be used directly as sensors [3, 4], in a fashion similar to piezoelectric films, or as a bias for sensors or power harvesters [5, 6].

When employed directly as a sensor element, geometrical alterations of the film change its electrostatic configuration. These changes can be amplified and recorded in applications such as strain sensing and inertial measurement. Although employed in a fashion similar to piezoelectric materials such as PZT, BaTiO<sub>3</sub>, and LiNbO<sub>3</sub>, polymer electrets offer advantages including process flows compatible with MEMS-friendly fabrication and options for conformal and transparent coating.

In addition, an electret can, through the large remnant voltage seen across its surface, be used as a permanent voltage bias within a sensor. This approach is used in the electret microphone, wherein the electret biases a movable diaphragm. Acoustic waves incident on the diaphragm move it with respect to the electret film, thereby creating a change in the electric field and a measurable output. Similarly, in energy harvesters, the electret film is often used to bias a mass that, when moves, leads to a current flow through an external circuit.

In these applications, the use of electret films leads to challenges in overall device fabrication. In particular, during the charging process, during which a polymer film is polarized, the surface of the polymer must be exposed to the charging apparatus. This provides a requirement that no structure be fabricated above the film prior to charging. Furthermore, once charged, the film will undergo significant discharge of temperatures near the glass transition of the polymer are seen. This limits further device fabrication to low-temperature processes.

As a result, most devices that employ active electret films are fabricated in two parts, one being a sensor component, and the other being a separate electret component. The electret can then be charged independently of the sensor fabrication.

After completing fabrication of the two parts, they are assembled using a low-temperature process. It is often desirable to fabricate the entire device on one wafer, however, and perform electret formation after wafer completion. *In situ* charging approaches can fulfill this desire.

## 2. ELECTRET INTEGRATION APPROACH

Figure 1 shows traditional electret charging based on the corona discharge apparatus. A needle with a 2 mm diameter tip is suspended 10 mm above the specimen. High voltage placed on the tip leads to ionization of the air near the tip. Charged species accelerate through a biased control grid towards the specimen, where they transfer charge to the surface. The large bulk resistivity of the polymer surface allows the charge to remain for long periods of time.

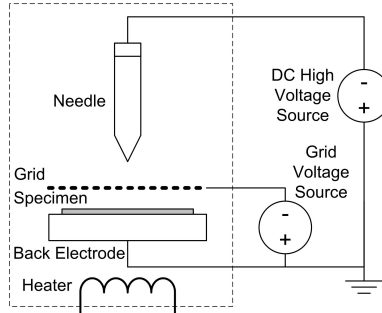


Figure 1: Schematic Corona Discharge System

Microcorona discharges have been previously achieved in microfabricated structures [7, 8, 9]. We demonstrate the use of this phenomenon for *in situ* charging of electrets and electret arrays. The *in situ* approach described here miniaturizes the traditional corona discharge apparatus, and embeds it within the sensor device itself. Figure 2 shows a cross-section of an *in situ* charging grid comprising multiple micro corona electrodes. These electrodes are conceptually similar to the corona wires in copy machines and laser printers. They are suspended above the electret film using posts fabricated from the film itself. When energized, dielectric breakdown of the air in the gap leads to plasma discharges resulting in charge transfer to the electret film. This charging grid can be fabricated within the MEMS structure itself and electret polarization can occur after complete device fabrication and release.

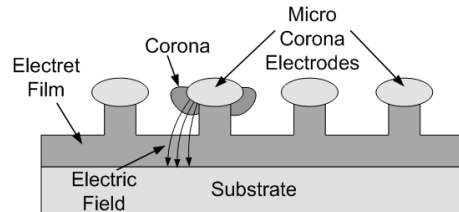


Figure 2: Miniature MicroCorona Sources

## 3. OPERATIONAL CONCEPT

Figure 3 illustrates how microcorona discharge would be employed within a sensor device. The sensor device under consideration consists of simple metal bridges suspended above a charging grid and polymer film. Once polarized, the electret film creates a voltage bias that capacitively couples with the suspended metal bridge. As the bridge experiences motion, a displacement current is generated in an external circuit.

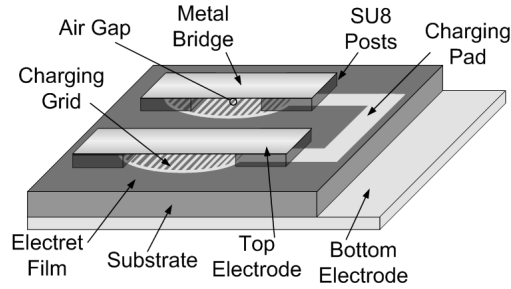


Figure 3: In situ Polarized Electret-Biased MEMS Sensor

CYTOP [10], a thermoplastic fluoropolymer encapsulant for electronics, is used as the polymer electret film because it can be spin-cast, has a high resistivity, and is easily etched in oxygen plasma. The grid structure is critical to the *in-situ* charging method. It consists of multiple thin-film metal edges suspended a short distance above the polymer film. When energized by a high voltage, the sharp metal edges lead to high dielectric fields that ionize the air in the gap and force electric charge onto the polymer surface. In this work, the grid consisted of an array of narrow lines, approximately  $5\mu\text{m}$  wide, and separated by an approximately  $40\mu\text{m}$  gap. The metal lines are suspended approximately  $2\mu\text{m}$  above the polymer film through the simple fabrication process shown in Figure 4. The metal is first deposited directly on the polymer, patterned, and then “suspended” by isotropically etching the polymer out from underneath it.

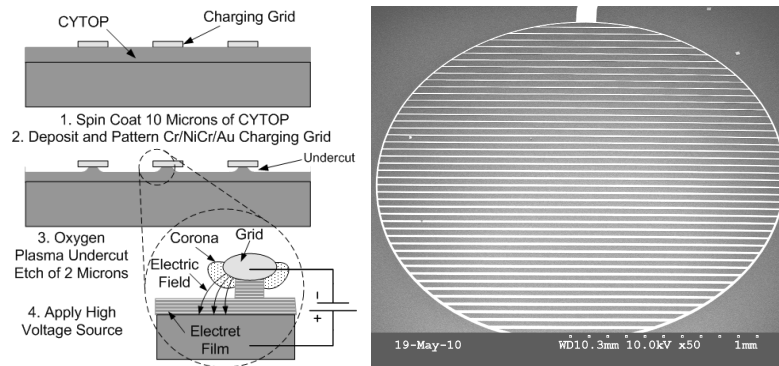


Figure 4: Fabrication Process and Fabricated Test Device for “Suspended” Charging Grid above Polymer Surface

After fabrication, the resulting grid structure is energized to a high voltage ( $\sim 800\text{V}$ ). The finite element model shown in Figure 5 illustrates the electric field distribution under the application of the potential. A cross-section of the electric field magnitude is shown on the right. As illustrated, a high electric field exists within the gap between the metal conductor and the polymer film. That electric field strength is greater than the dielectric strength of the air within the gap, leading to electrostatic discharge. However, the electric field decreases quickly enough that the field strength is less than the dielectric strength of the polymer film, thereby allowing the film to withstand the process.

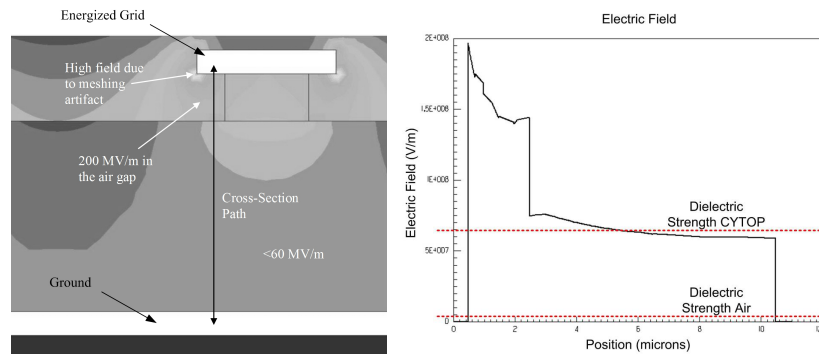


Figure 5: Fabrication Process for “Suspended” Charging Grid above Polymer Surface

## 4. IN SITU CHARGING

After the grid is fabricated, and any MEMS structures are built above it, the electret formation process is performed by energizing the grid to a high negative voltage. When a suitable potential is achieved across the air gap between the grid and the polymer film surface, a microcorona discharge occurs. Ions travel to the polymer surface where they transfer their charge. The charge builds up until sufficient potential is achieved such that the microcorona no longer exists. Figure 6 displays the current measured through the grid structure during the charging cycle. The first peak represents charge being placed on the grid to raise its potential. The second peak represents the increase in current due to the onset of the microplasma discharge. Figure 6 also illustrates a SPICE model developed to capture the features of this charging process. The model assumes that the system is in the Townsend Regime of electrostatic discharge. The current-voltage relationship in that regime is captured by the voltage source, V1, and the voltage-controlled resistor, U1. The threshold at which the initial formation of the microcorona discharge occurs is modeled by the switch, J1.

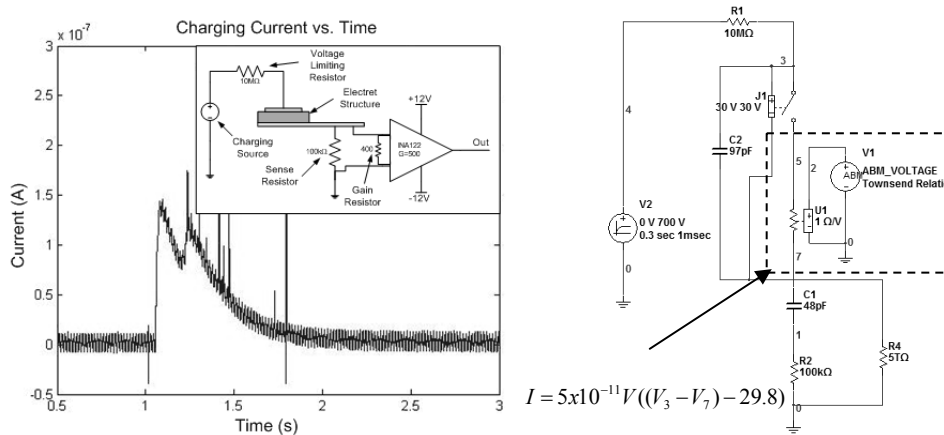


Figure 6: Measurement Circuit and Measured Current through the Structure during the First Charging Cycle

Figure 7 shows an optical image of the discharge event. The image on the left shows the charging grid as seen under normal lighting. The image on the right is of the same charging grid, but under no light conditions and captured during a portion of the discharge event. The intensity of the discharge is nonuniform across the charging grid and also time varying. This is due to nonuniformity of the metal edge sharpness, the orientation of the edge with respect to the polymer surface, and the actual gap between the edge and the polymer surface.

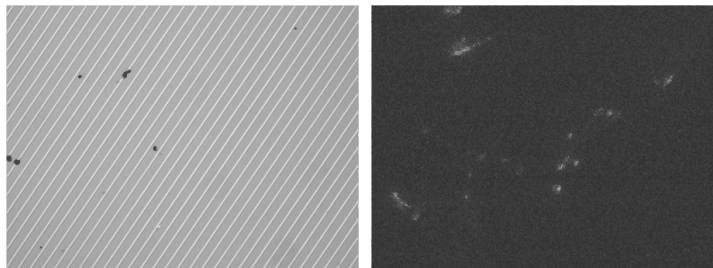


Figure 7: Optical Microscope Image of Discharge Process Showing Nonuniform Discharge Intensity

A field-nulling vibrating reed electrometer was used after polarization to measure the remnant voltage of each charging site. Figure 8 shows the achieved remnant voltage, after the application of -800V to the charging grid, plotted against the line spacing of the grid. Large line spacings resulted in higher remnant voltages as seen by the electrostatic voltmeter. This is due to the masking of the charge by the area of the metal conductors. The highest measured voltage results from the highest density of metal edges with the smallest total grid surface area.

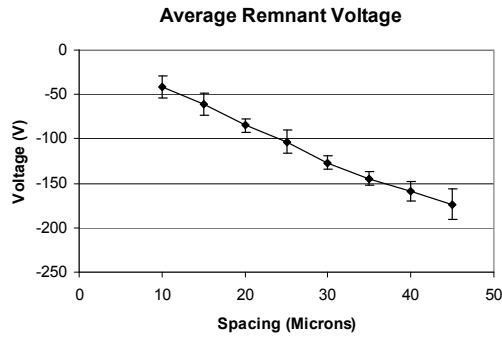


Figure 8: Average Remnant Voltage seen on Charged Sites of Varying Metal Spacing

Actual charged sites achieved an electrostatic voltage of approximately -200V after the first charging cycle when the grid was energized to -800V. Figure 9 shows the range of remnant voltages measured after polarizing multiple charging sites simultaneously on a single die. Each individual charging site is connected to the other charging sites and a contact pad. Upon application of the -800V charging potential, all sites are charged simultaneously.

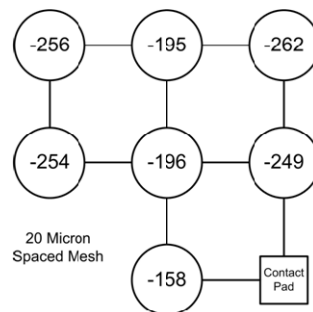


Figure 9: Remnant Voltages Measured for Multiple Simultaneous Charging Sites

## 5. SENSOR CHARACTERIZATION

Metal bridge transducer were suspended above an array charging sites; with each individual transducer in the array designed to exhibit a different natural frequency. This array was designed to perform spectral decomposition of an incident acoustic wave, with the natural frequencies spanning the range from 10kHz to 100kHz. When an impact or vibration is experienced, the output of the array represents a measurement of the spectrum of that input source. Figure 9 shows the sensor array attached to a hemispherical Alumina structure and impacted by a projectile. Four projectiles with identical geometries, but different materials, were dropped on to the hemisphere from a constant height. The materials used in the test were selected to provide a range of acoustic impedances, and included Teflon, acrylic, stainless steel, and silicon nitride.

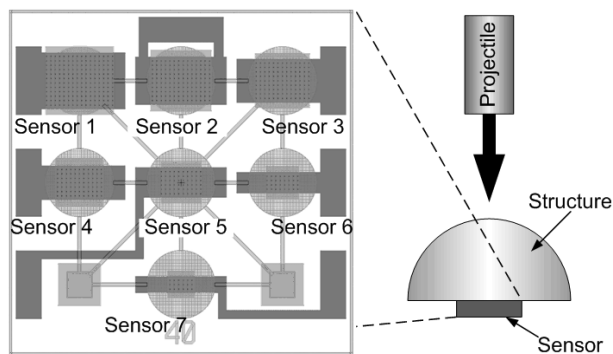


Figure 9: Sensor Array and Impact Test Setup

Figure 10 shows maximum peak voltage for each sensor from impacts between cylindrical projectiles of different materials and a ceramic hemi-sphere on which the sensor array is mounted. Each material presents a unique signature across the frequency spectrum. This sensor array demonstrates that *in situ* electret formation occurred within the structures, and that multiple sites could be charged with the application of voltage to a single contact pad, allowing the approach to be scaled to a full wafer implementation.

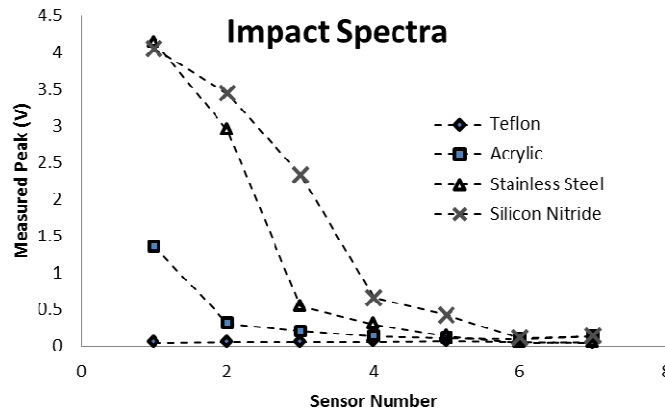


Figure 10: Output Spectra for Impacts with Different Materials

## 6. CONCLUSIONS

*In situ* charging of electret areas within a MEMS device is possible using microplasma discharges from a grid of thin film metal edges. The process can be performed after entire MEMS structure fabrication and release, thereby mitigating high-temperature process issues that electret films often experience. The process can also be scaled to the wafer-level.

## REFERENCES

- [1] Arakawa, Y., Suzuki, Y., and Kasagi, N., "Micro Seismic Power Generator Using Electret Power Film," *Power MEMS 2004*, Kyoto, Japan, Nov. 28, (2004).
- [2] Hsu, T. Y., Hsieh, W., and Tai, Y. C., "A Thin-Film Teflon Electret Technology for Microphone Applications," *Tech. Dig. Solid-State Sensors and Actuators Workshop*, (1996).
- [3] Goel, M., "Electret sensors, filters and MEMS devices: New challenges in materials research," *Current Science*, Vol. 85, No. 4, 25 August, (2003).
- [4] Hsu, T.-H., Yeh, C.-N., and Su, Y.-C., "Piezoelectric PDMS Electrets for MEMS Transducers," *IEEE MEMS 2010*, Hong Kong, January 25-28, (2010).
- [5] Sterken, T., Baert, K., Puers, R., Borghs, S., "Power extraction from ambient vibration," *Proceedings of the Workshop on Semiconductor Sensors*, November 29, (2002), Veldhoven, the Netherlands, p. 680-683.
- [6] Halvorsen, E., Westby, E. R., Husa, S., Vogl, A., Østbø, N.P., Leonov, V., Sterken, T., and Kvisterøy, T., "An Electrostatic Energy Harvester with Electret Bias," *Transducers 2009*, Denver, CO, June 21-25, (2009).
- [7] Lee, S., Kim, D., Bryant, M. D., Ling, F., "A Micro Corona Motor," *Sensors and Actuators A*, 118, (2005), pp. 226-232.
- [8] Wilson, C. G., and Gianchandani, Y. B., "Silicon Micromachining Using *In Situ* DC Microplasmas," *Journal of Microelectromechanical Systems*, Vol. 10, No. 1, March, (2001).
- [9] Honzumi, M., Ueno, A., Hagiwara, K., Suzuki, Y., "Soft-X-Ray-Charged Vertical Electrets and Its Application to Electrostatic Transducers," *23<sup>rd</sup> IEEE International Conference on MEMS (MEMS 2010)*, Hong Kong, January, (2010).
- [10] Sakane, Y., Suzuki, Y., and Kasagi, N., "The development of a high-performance perfluorinated polymer electret and its application to micro power generation," *Journal of Micromechanics and Microengineering*, 18 (2008) 104011 (6pp) 29 September 2008